Quasiresonance ionization of large multicharged clusters in a strong laser field

Isidore Last and Joshua Jortner
School of Chemistry, Tel-Aviv University, Ramat Aviv, Tel Aviv 69978, Israel
(Received 11 January 1999)

The high-order multielectron ionization of Xe_{531}, Xe_{1061}, and Xe_{2097} clusters in a strong laser field is studied using classical dynamics. The simulations are performed in the frozen geometry approximation for fixed ionic charges, so that only the evolution of the electrons, which are unbound to the ions, is examined. The dependence of the ionization efficiency on the laser frequency and cluster radius is manifested by pronounced maxima. The presence of these maxima favors the quasiresonance ionization mechanism, which is related to the motion of the unbound electrons in the entire cluster. The high level of ionization ($q \sim 8-18$ per atom) is realized in the expanded cluster, due to the Coulomb explosion. [S1050-2947(99)07408-9]

PACS number(s): 36.40.−c

I. INTRODUCTION

High levels of multielectron ionization of molecules and clusters are realized by photoionization in a strong laser field [1–13]. The multielectron ionization leads to a Coulomb explosion and to the production of multicharged atomic ions. Such an atomic ion production process is called multielectron dissociative ionization (MEDI). The kinetic energy of the product ions increases with the system size reaching ~1 MeV in large van der Waals (vdW) clusters composed of a few thousand atoms [6]. Another striking feature of the Coulomb explosion of large clusters is the generation of highly charged (up to Xe^{40+}) atomic ions [7].

The theoretical interpretation of the ionization processes in large clusters is of considerable interest. The quasistable plasma heating mechanism [10,12] provides a possible route for the ionization of large clusters. However, the existence of a quasistable plasma in multicharged large clusters at the time scale of several fs is questionable [14]. Before discussing the possible mechanism of large cluster ionization, it is useful to briefly describe the ionization mechanisms in small clusters and molecules. In valence diatomic molecules the multielectron ionization in a strong laser field is described by the charge resonance enhancement ionization (CREI) mechanism, which takes into account that the electron motion between two ions can be slowed down by an inner potential barrier [15–19]. This barrier rises with the interionic distance and at some distances the conditions for the enhancement of the electron energy are realized [15–19]. Due to this enhancement the electron energy may exceed the ionization potential (IP) of the system, which is mostly of the order of tens of eV, resulting in the ionization of the system. The MEDI process in small clusters composed of several atoms is characterized by higher levels of energies as compared to those of diatomic molecules [4,19,20]. For example, the IP of small multicharged rare-gas clusters Rg_n^{q+} ($n \approx 6-13$, $q \approx 4-8$) is of the order of ~100–200 eV. In spite of the large IP values, the MEDI process in small clusters may also be provided by the CREI mechanism, as was recently shown by us [19]. Interesting results pertain to the classical dynamics simulation of the MEDI process in Ar_6, Ar_{13}, and Ar_{55} clusters, recently performed by Ditmire [21]. According to these results, in small Ar_6 and Ar_{13} clusters the ionization of individual ions is quickly followed by the removal of electrons from the cluster, which is in line with the CREI mechanism. The picture is different in the intermediate size cluster Ar_{55} where the electrons removed from the individual ions are confined in and around the cluster for a relatively long time. Such behavior of the electrons contradicts the CREI mechanism and strongly indicates the presence of another ionization mechanism in large clusters.

In an intermediate ($n \sim 55$) or large size ($n > 100$) multicharged cluster the electrons are more strongly bound to the cluster than in a small ($n \leqslant 13$) cluster, so that they need considerably higher energy (roughly $E > 200$ eV for the charge $q \geqslant 2$ per atom) in order to leave the cluster. This energy may significantly exceed the height of the inner electrostatic barriers, which are similar to those in molecules and small clusters. Accordingly, these barriers, which are of prime importance in the CREI mechanism, cannot play any crucial role in the process of electron energy enhancement. This is probably the case with the Ar_{55} cluster, according to the results of Ditmire [21]. In a large multicharged cluster composed of about $\sim 10^3$ atoms, with the charge $q = 2-8$ per atom, the IP is of the order of a few KeV and consequently the energy of the electrons which leave the cluster is of the same magnitude. Since the motion of such highly energetic electrons cannot be hindered by any inner barriers, those energetic electrons are free to move inside the entire cluster. This motion may create the conditions for the enhancement of the electron energy, as was recently shown by us in the framework of a simple one-electron, one-dimensional model [14]. As in our previous work [14], the present study deals with the ionization of large xenon clusters Xe_n ($n = 500-2000$) to make contact with the experimental results of Hutchinson *et al.* [6–11]. Ionization dynamics in huge Xe_n clusters ($n \sim 10^5$), which results in nanoplasma formation of x-ray emission [22], is beyond the scope of the present study.

II. INNER AND OUTER IONIZATION

In treating the ionization process in large clusters, one has to distinguish between the inner and the outer ionization processes. Inner ionization corresponds to the removal of elec-

trons from their host atoms (ions) so that it determines the charge q_I of the cluster ions. Outer ionization is manifested by electron removal from the cluster to infinity so that it determines the total cluster charge Q or the charge $q=Q/n$ per atom and, consequently, the dynamics of the Coulomb explosion and the kinetic energy of the product atomic ions. The charges q_I, Q, and q are presented here in e-charge units and the number of unbound electrons per atom in the cluster is $n_e=\overline{q_I}-q$, $\overline{q_I}$ being the average ionic charge. The electrons generated by the inner ionization may continue their motion, leave the cluster, and go to infinity, which corresponds to a process of one-stage cluster ionization. However, the inner ionization may also result in the generation of unbound (delocalized) electrons, which oscillate for some time inside the cluster or in its vicinity. In this case the outer ionization is expected to be realized by the removal to infinity of these unbound electrons representing a process of two-stage cluster ionization.

In a strong outer field the ionization of neutral atoms and weakly charged ions can be realized by the suppression of the inner electrostatic barriers of these atoms and ions [23,24]. Some of the electrons, which are removed from their host atoms (ions), can also leave the cluster if the outer electrostatic barrier, which is formed in the vicinity of a charged cluster, is suppressed as well. The approximate condition for the suppression of the outer electrostatic barrier is

$$Q \leqslant \frac{1}{B} R^2 e F_0, \tag{1}$$

where Q is the total cluster charge, R is the cluster radius (in Å), eF_0 is the force amplitude (in eV/Å) of the outer (laser) field F, and $B=14.385$ eV/Å [14]. When Eq. (1) is fulfilled, the inner ionization is immediately followed by the outer ionization realizing the one-stage process of cluster ionization. In the Xe_{1100} cluster, for example, Eq. (1) provides $Q \leqslant 1190$ for the force amplitude $eF_0=27.4$ eV/Å [14]. It follows that the Xe_{1100} cluster loses its first ~ 1100 electrons (i.e., about one electron per atom) by the suppression of both inner and outer electrostatic barriers.

After a cluster becomes initially charged (most probably due to the suppression of the electrostatic barriers) the inner ionization may be provided by the ignition mechanism [25,26]. This mechanism takes into account that in a charged cluster there is an inner Coulomb field, which may remove electrons from ions by suppressing their inner electrostatic barriers. In a uniformly charged cluster this field points toward the cluster center and it is proportional to the total cluster charge Q. Consequently, the level of the inner ionization depends on the level of the outer cluster ionization, namely the higher the charge Q is, the larger the ionic charges q_I are. For example, according to our analysis, which was performed for the charged Xe_{1100} cluster in the geometry of a neutral cluster, most of the cluster atoms are deprived of their $5p$ electrons ($q_1=6$) when the initial total cluster charge is $Q \approx 1100$ ($q \approx 1$ per atom) [14]. When the cluster charge increases to $Q \approx 2640$ ($q \approx 2.4$ per atom), the ions located at the periphery are deprived of their two $5s$ electrons, becoming highly charged Xe^{8+} ions. Further increase in the cluster charge results in the removal of the xenon $4d$ electrons [14].

If there is an effective mechanism of outer ionization, then the unbound electrons generated by the ignition mechanism are removed from the cluster, realizing the two-stage process of cluster ionization. The outer ionization increases the cluster charge and consequently strengthens the inner ionization, which generates new unbound electrons for the outer ionization process. Such a two-stage ionization process prevails when both the inner and outer ionizations are in progress. When the efficiency of either inner or outer ionization is terminated, the process of electron removal from the cluster is switched off. The aim of the present study is to establish spatial, charge, and temporal limits for the cluster ionization process.

The cluster ionization described above takes into account only the ignition mechanism for the inner ionization. In addition to the ignition mechanism, the inelastic collision of energetic unbound electrons with ions may contribute to the inner ionization. The importance of the collisional ionization will be discussed in the next section.

The complete simulation of the ionization process has to treat both inner and outer ionizations. It also has to treat the nuclear dynamics of the Coulomb explosion [2,20,27]. The consideration of these electronic and nuclear processes requires the treatment of the motion of three kinds of particles: the electrons bound to host ions, the unbound electrons, and the heavy particles (ions). The most complicated problem corresponds to the treatment of the inner ionization since the motion of the bound electrons inside ions (atoms) is of pronounced quantum origin. In the available dynamical simulations of the cluster ionization, the bound electrons are not treated at all, and the inner ionization is described as the generation of unbound electrons by ions (atoms) when the conditions for inner ionization are fulfilled [21,26]. The aim of the present work is to study the outer ionization process by treating the dynamics of the cluster unbound electrons.

III. CLASSICAL DYNAMICS SIMULATION OF THE IONIZATION PROCESS

In this work we study the ionization process in large van der Waals clusters consisting of hundreds or thousands of atoms. In order to simplify the simulation of such large clusters, we decided to incorporate into our treatment a number of approximations. We restrict our treatment to the problem of the outer ionization of unbound electrons. It is expected that these electrons are generated by the inner ionization process, but this process will not be considered in our simulation. Some estimates of the inner ionization efficiency will be given in the Appendix. In the present study we shall not perform the simulation of the Coulomb explosion dynamics. We do account, however, for the effects of Coulomb explosion by performing the simulation at different frozen nuclear configurations.

Consequently, we are only left with the problem of the motion of the unbound electrons, both when linked to the cluster and when removed from it. The number of these electrons is assumed to be fixed in the time of the dynamic simulations. The inelastic scattering of the unbound electrons by ions and, in particular, the collisional ionization of these ions, is neglected. These approximations impose serious restrictions on the problems which are treated by our dynamic

simulations. In particular, dealing with unbound electrons only, we imply the two-stage ionization process. Consequently, we cannot study the cluster ionization from the very beginning when the cluster is neutral or weakly charged and the cluster ionization corresponds to a one-stage process.

In a strong laser field an electron gains enough energy to ionize neutral atoms or weakly charged ions [28]. Since we neglect the collisional ionization of ions by energetic unbound electrons, we have to exclude from our treatment the clusters where this ionization process is of importance. The collisional ionization cross section σ can be estimated by Lotz's expression [29]. As applied to the ionization of the i-fold ($i=q_I$) ionized ion, this expression is

$$\sigma_i = a\sum_{j=i}^{J} (1/KI_j)\ln(K/I_j), \tag{2}$$

where $a=450\,(\mathrm{eV})^2\,\text{Å}^2$, K is the kinetic energy of the impact electron, I_j is the ionization potential of the j-fold ionized ion ($j\geqslant i$), and $I_J<K<I_{J+I}$. The σ_i dependence on K demonstrates a maximum:

$$(\sigma_i)_{\max} = \frac{a}{I_i e^{\gamma}}\sum_{j=i}^{J} (1/I_j), \tag{3}$$

where

$$\gamma = 1+\left(\sum_{j=i+1}^{J} (1/I_j)\ln(I_j/I_i)\right) \Big/ \sum_{j=i}^{J} (1/I_j). \tag{3'}$$

The upper limit J of the summarization in expressions (3) is determined by the inequalities

$$\sum_{j=i}^{J} (1/I_j)[1-\ln(I_J/I_j)]>0,$$

$$\sum_{j=i}^{J+1} (1/I_j)[1-\ln(I_{J+1}/I_j)]<0. \tag{4}$$

The kinetic energies K of the unbound electrons in the cluster are expected to be widely spread so that it is not useful to estimate σ for concrete K values. Taking this into account, we estimate only the maximal cross sections here [presented by Eq. (3)] and consequently the lower limits of the collisional ionization free paths $l_{\min}=(\sigma_{\max}N_a)^{-1}$, with $N_a=0.017\,\text{Å}^{-3}$ being the atomic density of the Xe_n clusters. In the case of the Xe^+ ion ($q_I=i=1$), the free path was found to be $l_{\min}=90$ Å. This l value is comparable to the cluster diameter, which in the $n\sim1000$ cluster is $2R_c\approx50$ Å. It indicates the effective contribution of the collisional ionization process in a cluster composed of single charged ions. The collisional ionization free path increases to $l_{\min}=810$ Å for the Xe^{5+} ion ($5p5s^2$ outer shell) and to $l_{\min}=1600$ Å for Xe^{6+}
($5s^2$ outer shell). In the case of the Xe^{5+} ion, the condition $l\gg2R_c$ is fulfilled and the ionization probability during one cluster crossing is really very small. However, since the characteristic frequency of motion of the unbound electrons in a multicharged cluster is about 1 fs^{-1}, an unbound electron may cross the cluster more than 10 times before leaving it [14]. Consequently, in Xe^{5+} clusters the collisional ionization may be of some importance, although we expect it to be limited. In clusters composed of Xe^{6+} and of higher charge ions, the collisional ionization may most probably be neglected, so we decided to restrict our treatment to clusters with ionic charge $q_I\geqslant6$ per atom.

In our approach, the dynamics simulation only allows us to study the effect of laser field and cluster parameters on the outer ionization efficiency and to analyze the mechanism of this ionization. In order to mimic the Coulomb explosion in the framework of the frozen geometry approach, the dynamics simulation was performed not only for the neutral cluster geometry but also for expanded geometries. We suggest here that the ignition mechanism of the inner ionization is sufficiently effective to provide unbound electrons. This suggestion imposes restrictions on the cluster size since the efficiency of the ignition mechanism becomes low in small clusters composed of several or tens of atoms. In our treatment we consider clusters composed of hundreds or thousands of atoms where the ignition mechanism, according to our analysis, is highly effective (see the Appendix).

In treating the dynamics of unbound electrons, one needs to take into account the electron-electron interaction and the electron interaction with the ions and with the outer (laser) field. In order to prevent a steep increase in the electron-electron repulsion forces at very small distances r, which may result in the violation of energy conservation, a smoothing term is included into the electron-electron potential:

$$U_{e\text{-}e} = \frac{B}{\sqrt{r^2+r_0^2}}. \tag{5}$$

The smoothing parameter of the potential (5) is taken as $r_0^2=0.37\,\text{Å}^2$. This value was chosen as the minimal smoothing parameter which does not violate the energy conservation.

The potential of the electron-ion interaction is expressed as a sum of the Coulomb attractive potential and a short-range repulsive term

$$U_{e\text{-}I} = -\frac{Bq_I}{r}+\frac{C}{r^{\eta}}. \tag{6}$$

The task of the repulsive term with $\eta=6$ is dual: it prevents the electron penetration into the region of very high Coulomb forces, which may result in the violation of the energy conservation, and simulates the elastic scattering of the unbound electrons on ion electrons. Here we do not apply the exponential repulsive term, which is used in the case of electron-neutral atom interaction [30,31], since in the case of multicharged ions such a term may not prevent the penetration of energetic electrons into the region of very high Coulomb forces. The short-range $1/r^6$ term prevents such a penetration and provides the energy conservation. Unfortunately, direct data concerning the repulsive term in the electron-multicharged ion interaction are not available. We can get some idea about the range of the repulsive term from the size of the outer electronic shell of the ion. The size of the electronic shells can be estimated, although very roughly, by using the Slater rules [32]. These rules provide the average radius $r_{\text{av}}=\langle r^2\rangle^{1/2}=1.66$ Å for the outer $5s$ orbital of the Xe^{6+} ion. Taking into account the presence of

two $5s$ electrons in the Xe^{6+} ion, we suggest that the total force of the potential [Eq. (6)] becomes zero ($dU_{e-I}/dr=0$) at a distance $r_0=1.15\,r_{\rm av}$. This condition provides $C=410\,\text{eV}\,\text{Å}^6$. In the Xe^{8+} ion the average radius of the outer shell $4d$ is very small, $r_{\rm av}=0.67$ Å, so that the elastic scattering is expected to be negligible. As mentioned above, the repulsive term cannot be neglected because of the problems of energy conservation. However, in order to avoid the violation of energy conservation, we introduce a repulsive term with a small coefficient of $C=36\,\text{eV}\,\text{Å}^6$ in the case of the Xe^{8+} ion, as well as for ions with higher charge. According to our calculations, the dynamics simulation results depend weakly on the C parameter.

The outer laser field force is

$$eF=eF_0\cos(2\pi\nu t+\varphi_0), \tag{7}$$

where F is the field strength, ν is the laser light frequency, and φ_0 is the initial phase. In the present dynamic simulations the laser light power is constant and equal to $10^{16}\,\text{W/cm}^2$, which corresponds to the field force amplitude of $eF_0=27.45\,\text{eV/Å}$. There is no need to take the real shape of the laser pulse into account as the simulation is performed here for relatively short time intervals, mostly 10 fs, and without considering the initial stages of the laser irradiation when the laser pulse power increases sharply.

IV. SIMULATIONS RESULTS

Dynamic simulations have been performed for multicharged clusters Xe_{531}, Xe_{1061}, and Xe_{2093} (neutral cluster radii $R_0=18.9$, 24.5, and 30.4 Å, respectively, interatomic distance $d=4.33$ Å) and in a wide range of ionic charges ($q_I=6-30$) and cluster expansion radii ($R/R_0=1-4$). The cluster of a given radius is assumed to be of a uniform density, in spite of the fact that in the expanded cluster the density is smaller on the periphery than in the center due to Coulomb explosion [20]. It is also assumed that all ions bear the same fixed charge q_I and that the unbound electrons are initially distributed, at $t=0$, inside the cluster in a uniform way and with zero kinetic energy. It is important to note that the initial condition $t=0$ does not mark the beginning of the cluster irradiation but rather the onset of the dynamic processes in an initially ionized cluster. Taking the electron energy to be zero at $t=0$, we neglect the heating of these electrons during the previous period of cluster irradiation.

The ionization rates are given by the number of removed electrons per fs during the first 10 fs of the simulation. When the ionization rate varies strongly during the simulation time, the maximal ionization rate value is taken as the representative value. The dependence of the ionization rates on the laser light frequency ν is presented in Fig. 1 for Xe_{531} and Xe_{1061} clusters. The most interesting feature of the data presented in Fig. 1 is manifested by the pronounced maxima in the ionization rates. The increase of the cluster radius shifts these maxima to lower frequencies and increases their height. When the cluster radius R is twice as large as the neutral geometry radius R_0, the ionization rates in the Xe^{8+} clusters become large, with about 350–450 electrons being removed per fs [Fig. 1(b)]. The ionization rates in the Xe_{1061} and Xe_{531} clusters are similar. The comparison of the Xe_{531}

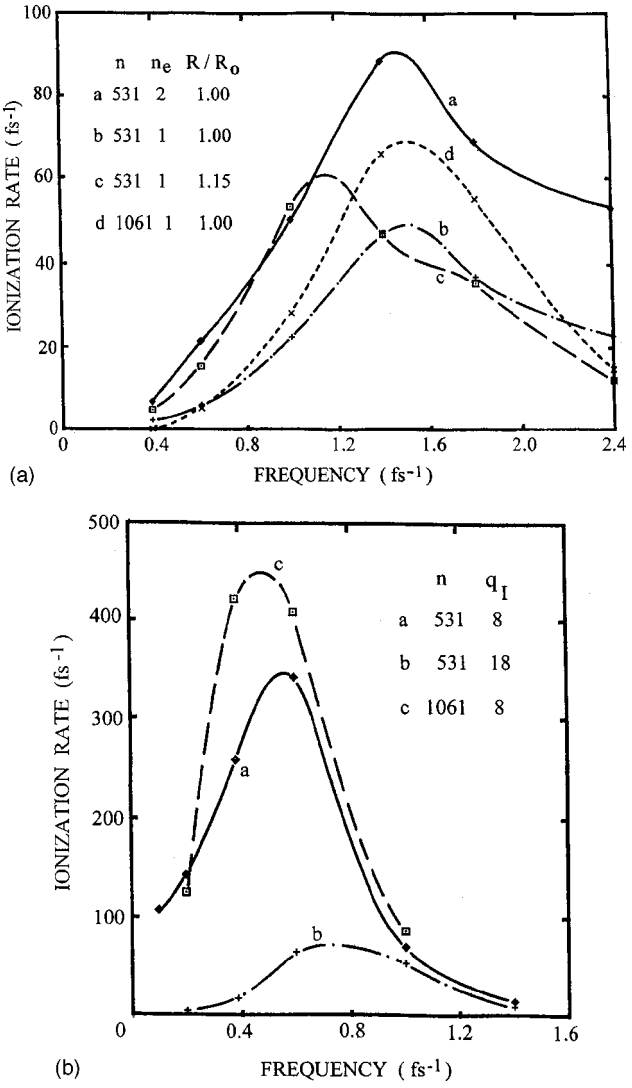

FIG. 1. The ionization rate dependence on laser frequency ν for Xe_n ($n=531,1061$) clusters. The ionization rate is determined as the number of electrons removed from the cluster in 1 fs (see text). q_I, ions charge; n_e, the initial number of unbound electrons per atom; R/R_0, cluster radius in units of the neutral cluster radius R_0. (a) $q_I=8$, (b) $n_e=1$, $R/R_0=2$.

$q_I=8$ ionization rates for the number of unbound electrons $n_e=2$ and $n_e=1$ per atom [Fig. 1(a)] shows that the ionization rate is roughly proportional to n_e. In the geometry of a neutral cluster ($R=R_0$) the ionization rate maxima lie in the UV region, i.e., $\nu\approx 1.4\,\text{fs}^{-1}$ [Fig. 1(a)]. In the IR frequency interval of $\nu=0.3-0.4\,\text{fs}^{-1}$, where cluster ionization experiments are usually performed, the ionization efficiency is very low. Only after the cluster expands to the radius $R=2R_0$ are the maxima shifted to the IR region and the ionization rate becomes very high [Fig. 1(b)]. In the Xe_{2093} cluster the ionization efficiency is high in the expanded geometry of $R=2R_0$ for $q_I=8$ and $R=2.8R_0$ for $q_I=18$, as in the Xe_{531} and Xe_{1061} clusters.

The dependence of the ionization efficiency on the cluster radius R is presented in Fig. 2 for the laser light frequency of $\nu=0.386\,\text{fs}^{-1}$ (such laser frequency was used in the cluster ionization experiments of Ref. [10]). The ionization efficiency of Fig. 2 is determined as the percentage of unbound

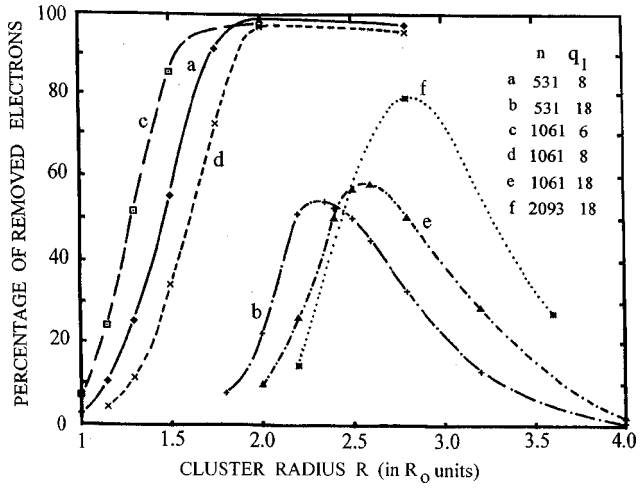

FIG. 2. The ionization level dependence on the cluster radius R/R_0 (see caption of Fig. 1). The ionization level is presented as the percentage of the unbound electrons removed from the cluster in the first 10 fs of the simulation. The initial number of unbound electrons is $n_e=1$ per atom, the laser frequency being $\nu=0.386\,\mathrm{fs}^{-1}$.

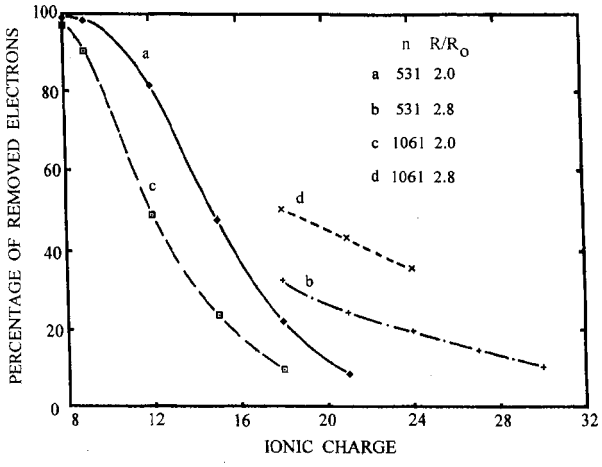

FIG. 3. The ionization level dependence on the ions charge q_I for $n_e=1$ and $\nu=0.386\,\mathrm{fs}^{-1}$ (see captions of Figs. 1 and 2).

electrons, which are removed from the cluster during the first 10 fs of the simulation. As in the case of the ionization rate frequency dependence (Fig. 1), the ionization efficiency size dependence also shows maxima, at least in highly charged clusters composed of Xe^{18+} ions. The clusters composed of Xe^{6+} and Xe^{8+} ions do not show maxima (Fig. 2) since they exhibit saturation effects at large R, with their ionization efficiency being close to 100% in a wide interval of the cluster radii R.

The presence of maxima in the ionization rate dependence on light frequency (Fig. 1) and in the ionization efficiency dependence on the cluster radius (Fig. 2) strongly favors the quasiresonance mechanism for the ionization of large clusters. The physical interpretation of the quasiresonance ionization (QRI) mechanism in these clusters is straightforward. In the absence of the outer field, the unbound electrons of large multicharged clusters oscillate inside the entire cluster. When the average frequency ν_e of the electron oscillations in the entire cluster is close to the light frequency ν, the quasiresonance conditions are met and the energy of electrons is enhanced resulting in the increase of the outer ionization efficiency. According to our results for the light frequency $\nu=0.386\,\mathrm{fs}^{-1}$ (Fig. 2), the ionization efficiency is low at the initial geometry of the neutral cluster, since in this geometry $\nu_e \gg \nu$ and the quasiresonance conditions are not fulfilled. However, after the cluster becomes initially ionized, its radius R begins to increase, due to the Coulomb explosion, which results in the decrease in the electron frequency ν_e. At some radius R, when the quasiresonance conditions are satisfied ($\nu_e \sim \nu$), the outer ionization efficiency becomes high. In the case of strongly charged ions with $q_I=18$, for example, the ionization efficiency maxima are reached at $R\approx 2.2$, 2.5, and 2.9 Å for Xe_{531}, Xe_{1061}, and Xe_{2091} clusters, respectively (Fig. 2). Such increase in the cluster size may occur, according to our estimates, on the time scale of 15–25 fs [14,19].

The decrease of the electron oscillation frequency ν_e, which leads to the quasiresonance energy enhancement, is caused in large clusters by the decrease of the cluster charge density and the increase of the electron oscillations amplitude. Such a mechanism of energy enhancement is completely distinct from that of the CREI mechanism, which considers the electron oscillations between neighboring ions and contributes the decrease of the frequency ν_e of these oscillations to the effect of the inner potential barrier [17–19].

The dependence of the ionization efficiency on the ionic charge q_I is presented in Fig. 3. The ionization efficiency was found to decrease slowly in the region of large q_I, so that even highly charged clusters composed of ions with $q_I=20-30$ may still lose unbound electrons. Our results, however, do not answer the question of whether such highly charged ions can really be provided by the inner ionization. In order to answer this question, we estimated the limits of the inner ionization efficiency. According to our estimates, performed in the Appendix, the maximal charges of the ions produced by the ignition mechanism of the inner ionization are moderately low. In the case of the Xe_{1061} cluster in the expanded geometry radius $R=2R_0$, for example, the maximal ionic charge is $q_I=10$ (see the Appendix), whereas the outer ionization is still effective for much higher ionic charges of $q_I\approx 18$ (Fig. 3). A further increase in the cluster size, which leads to the increase of the outer ionization efficiency (Fig. 2), diminishes the inner ionization efficiency. It follows that the inner ionization constitutes the ''bottleneck'' for the cluster ionization process.

ACKNOWLEDGMENT

This research was supported by the Binational German-Israeli James Franck program on Laser-Matter Interaction.

APPENDIX

We will estimate the limits of the inner ionization provided by the ignition mechanism. The condition of the inner ionization, according to the ignition mechanism, is the suppression of a potential barrier which keeps an electron inside its host ion [25]. In the i-fold ionized ion this barrier is suppressed if the absolute value of the inner potential maximum U_i is larger than the ionization potential I_i:

$$|(U_i)_{\max}| > I_i . \tag{A1}$$

In order to find $(U_i)_{\max}$, let us consider a bound electron located on a line which connects its host ion with the cluster center. In the case of a uniformly charged cluster (total charge $Q=nq$) and the outer (laser) field $F=F_0$ directed toward the cluster center, the potential of this electron is

$$U(r) = -\frac{Bq_I}{r} - \frac{BQ_I}{R_I^2} r - eF_0 r, \tag{A2}$$

where r is the electron-host ion distance, $q_I=i+1$ is the host ion charge (after the electron is removed), R_I is the host ion distance from the cluster center, and Q_I is the total charge of ions and unbound electrons located inside the R_I radius sphere. Eq. (A2) implies $r \ll R_I$. Assuming the distance r to be small compared to the interionic distance d ($r \ll d$), where the interionic distance is much smaller than R_I ($d \ll R_I$), the charge Q_I can be approximately expressed as

$$Q_I = nq\left(\frac{R_I}{R}\right)^3\left(1-\frac{d}{2R_I}\right)^3, \tag{A3}$$

where R is the cluster radius. Assuming also that the outer field eF_0 is much smaller than the one generated by the charge Q_I field, we obtain the following expression for the maximum of the potential in Eq. (A2):

$$|U_{\max}| = \frac{2B\sqrt{nqq_I}}{R}\left(\frac{R_I}{R}\right)^{1/2}\left(1-\frac{3d}{4R_I}+f\right), \tag{A4}$$

where

$$f = \frac{eF_0R^3}{2BnqR_I}. \tag{A5}$$

The estimates of the maximal ionization levels which satisfy the criterion (A1) were performed for the Xe_{1061} cluster with the charge $q=q_I-1$ per atom (the number of unbound electrons $n_e=1$ per atom). The ionization potentials I_i were taken from Refs. [33,34].

According to our estimates, in the neutral cluster geometry the maximal ion charge which satisfies the criterion (A1) is as large as $q_I=24$. However, the cluster cannot be strongly ionized at $R=R_0$ (Fig. 2). Only at $R>R_0$ does the efficiency of the outer ionization begin to increase, but at the same time the maximal ion charge q_I provided by the criterion (A1) decreases. Thus it is $q_I=14$ and $q_I=10$ for $R=1.5R_0$ and $R=2R_0$, respectively.

Our estimates are based on the assumption of the uniform distribution of the cluster charge. Fluctuations of the charge distribution may contribute to a little higher level of inner ionization. High-level inner ionization may be provided by collisional electron ionization, however the cross section of this process for highly charged ions is very small [see Eq. (3)].

[1] K. Codling, L. J. Frasinski, P. Hatherly, and J. R. M. Barr, J. Phys. B **20**, L525 (1987).
[2] K. Boyer, T. S. Luk, J. C. Solem, and C. K. Rhodes, Phys. Rev. A **39**, 1186 (1989).
[3] D. Normand and M. Schmidt, Phys. Rev. A **53**, R1958 (1996).
[4] J. Purnell, E. M. Snyder, S. Wei, and A. W. Castleman, Jr., Chem. Phys. Lett. **229**, 333 (1994).
[5] J. Kou, N. Nakashima, S. Sakabe, S. Kawato, H. Ueyama, T. Urano, T. Kuge, Y. Izawa, and Y. Kato, Chem. Phys. Lett. **289**, 334 (1998).
[6] T. Ditmire, J. W. G. Tisch, E. Springate, M. B. Mason, N. Hay, R. A. Smith, J. Marangos, and M. H. R. Hutchinson, Nature (London) **386**, 54 (1997).
[7] T. Ditmire, J. W. G. Tisch, E. Springate, M. B. Mason, N. Hay, J. P. Marangos, and M. H. R. Hutchinson, Phys. Rev. Lett. **78**, 2732 (1997).
[8] T. Ditmire, R. A. Smith, J. W. G. Tisch, and M. H. R. Hutchinson, Phys. Rev. Lett. **78**, 3121 (1997).
[9] Y. L. Shao, T. Ditmire, J. W. G. Tisch, E. Springate, J. P. Marangos, and M. H. R. Hutchinson, Phys. Rev. Lett. **77**, 3343 (1996).
[10] M. H. R. Hutchinson, T. Ditmire, E. Springate, J. W. G. Tisch, Y. L. Shao, M. B. Mason, N. Hay, and J. P. Marangos, Philos. Trans. R. Soc. London, Ser. A **356**, 297 (1998).
[11] T. Ditmire, E. Springate, J. W. G. Tisch, Y. L. Shao, M. B. Mason, N. Hay, J. P. Marangos, and M. H. R. Hutchinson, Phys. Rev. A **57**, 369 (1998).
[12] T. Ditmire, T. Donnelly, A. M. Rubenchik, R. W. Falcone, and M. D. Perry, Phys. Rev. A **53**, 3379 (1996).
[13] M. Lezius, S. Dobosh, D. Normand, and M. Schmidt, Phys. Rev. Lett. **80**, 261 (1998).
[14] I. Last and J. Jortner, J. Phys. Chem. **102**, 9655 (1998).
[15] T. Zuo, S. Chelkowski, and A. D. Bandrauk, Phys. Rev. A **48**, 3837 (1993).
[16] T. Zuo and A. D. Bandrauk, Phys. Rev. A **52**, R2511 (1995).
[17] S. Chelkowski and A. D. Bandrauk, J. Phys. B **28**, L723 (1995).
[18] T. Seideman, M. Yu. Ivanov, and P. B. Corkum, Phys. Rev. Lett. **75**, 2819 (1995).
[19] I. Last and J. Jortner, Phys. Rev. A **58**, 3826 (1998).
[20] I. Last, I. Schek, and J. Jortner, J. Chem. Phys. **107**, 6685 (1997).
[21] T. Ditmire, Phys. Rev. A **57**, R4094 (1998).
[22] S. Dobosh, M. Lezius, M. Schmidt, P. Meynadier, M. Perdix, D. Normand, J.-P. Rozet, and D. Vernhet, Phys. Rev. A **56**, R2526 (1997).
[23] S. Augst, D. Strickland, D. Meyerhofer, S. L. Chin, and J. H. Eberly, Phys. Rev. Lett. **63**, 2212 (1989).
[24] H. Yu, T. Zuo, and A. D. Bandrauk, J. Phys. B **31**, 1533 (1998).
[25] C. Rose-Petruck, K. J. Schafer, and C. P. J. Barty, Proc. SPIE **2523**, 272 (1995).
[26] C. Rose-Petruck, K. J. Schafer, K. R. Wilson, and C. P. J. Barty, Phys. Rev. A **55**, 1182 (1997).
[27] J. Jortner and R. D. Levine, Isr. J. Chem. **30**, 207 (1990).
[28] A. D. Bandrauk and H. Yu, Phys. Rev. A **59**, 539 (1999).
[29] W. Lotz, Z. Phys. **216**, 241 (1968).

[30] P. E. Siska, J. Chem. Phys. **71**, 3942 (1979).
[31] I. Last and T. F. George, J. Chem. Phys. **98**, 6406 (1993).
[32] C. A. Coulson, *Valence* (Oxford University Press, Oxford, 1961).
[33] R. D. Cowan, *The Theory of Atomic Structure and Spectra* (University of California Press, Berkeley, 1981).
[34] T. A. Carlson, C. W. Nestor, Jr., N. Wasserman, and J. D. McDowell, At. Data **2**, 63 (1970).